J Fluoresc (2014) 24:1581–1591
DOI 10.1007/s10895-014-1441-9

ORIGINAL PAPER

Novel Photochrome Aptamer Switch Assay (PHASA) for Adaptive Binding to Aptamers

Vladislav Papper · Oleksandr Pokholenko · Yuanyuan Wu · Yubin Zhou · Ping Jianfeng · Terry W. J. Steele · Robert S. Marks

Received: 5 August 2014 / Accepted: 11 August 2014 / Published online: 5 September 2014

Abstract A novel Photochrome-Aptamer Switch Assay (PHASA) for the detection and quantification of small environmentally important molecules such as toxins, explosives, drugs and pollutants, which are difficult to detect using antibodies-based assays with high sensitivity and specificity, has been developed. The assay is based on the conjugation of a particular stilbene-analyte derivative to any aptamer of interest. A unique feature of the stilbene molecule is its reporting power via *trans-cis* photoisomerisation (from fluorescent *trans*-isomer to non-fluorescent *cis*-isomer) upon irradiation with the excitation light. The resulting fluorescence decay rate for the *trans*-isomer of the stilbene-analyte depends on viscosity and spatial freedom to rotate in the surrounding medium and can be used to indicate the presence of the analyte. Quantification of the assay is achieved by calibration of the fluorescence decay rate for the amount of the tested analyte. Two different formats of PHASA have been recently developed: direct conjugation and adaptive binding. New stilbene-maleimide derivatives used in the adaptive binding format have been prepared and characterised. They demonstrate effective binding to the model thiol compound and to the thiolated Malachite Green aptamer.

Keywords Stilbene · Aptamer · Fluorescence · Photoisomerisation · Maleimide

Abbreviations

2b	4-methoxy-4′-stilbene maleimide
2a	4-*N,N*′-dimethylamino-4′-stilbene maleimide
MG	Malachite green
DMSO	Dimethyl sulfoxide
DMF	Dimethyl formamide
MCH	6-mercaptohexanol
EX	Fluorescence excitation
EM	Fluorescence emission

Introduction

As one of the simplest means of converting light into mechanical motion on the angstrom scale, photo-induced *trans-cis* isomerisation about double bonds has long been a subject of thorough research. The mechanisms of the photoisomerisation of 1,2-diphenylethenes, or stilbenes, and their derivatives have been intensively discussed in literature [1–4]. The conventional picture of this process has been simplified as a two-state, one-dimensional model, stressing torsional motion as the primary nuclear coordinate.

So far, stilbene compounds have never been successfully used as the molecular sensing entities in the biosensing devices and bioassays, although they possess all the desired features of the ideal reporter molecules, for instance, chemical and biological stability, relatively low toxicity, synthetic availability, high photochemical sensitivity, rapid response and easy regeneration. This is mainly because of their strong tendency to rapidly lose fluorescence upon excitation via the non-radiative deactivation process connected to the twisted transition in the excited state [1–4]. The latter is responsible

Vladislav Papper and Oleksandr Pokholenko contributed equally to this manuscript.

V. Papper · O. Pokholenko · Y. Wu · Y. Zhou · P. Jianfeng · T. W. J. Steele (✉)
School of Materials Science and Engineering, Nanyang Technological University, Singapore 639798, Singapore
e-mail: wjsteele@ntu.edu.sg

R. S. Marks
Department of Biotechnology Engineering, National Institute for Biotechnology in the Negev, Ilse Kats Institute for Nanoscale Science and Technology, Ben Gurion University of the Negev, Beer Sheva, Israel

for the *trans-cis* photoisomerisation of the molecule and acts as a quenching funnel on fluorescence emission, thereby depriving the fluorescence probe of its photochemical stability.

Thus, as schematically pictured on Fig. 1a, many stilbene compounds can rapidly change their molecular configuration upon irradiation at the excitation maximum, if they are not sterically and electronically restricted to do so. The *trans-cis* photoisomerisation process is experimentally observed at the constant-illumination conditions as the rapid steady-state fluorescence decay to the photostationary equilibrium between the two isomers. Such photochemical instability could be a huge problem if the stilbene compound is considered a fluorescence probe. And this is probably the reason why the stilbene compounds have never been effectively used in biomedical applications. However, the actual reporting power of the stilbenes is not in their fluorescence, but in rapid loss of their fluorescence via an instant conformational change upon irradiation with the excitation light. This makes the stilbene switches unique in the sense that most fluorescent reporters (labels or probes) either do not possess this intramolecular switchable nature or require the separation of adjacent fluorophores.

In view of the above, one of the most striking features of stilbene photochemistry is its essentially strong dependence on medium microviscosity. We have previously provided clear evidence that the *trans-cis* photoisomerisation of stilbene compounds is very sensitive to medium microviscosity and can be used in biomedical applications [5–8]. The new fluorescence-photochrome method, developed by us, was used for investigation of local medium effects and phase transitions in biological membranes and on solid surfaces [5–8]. The method is based on monitoring the *trans-cis* photoisomerisation kinetics of stilbenes incorporated into an object of interest. It has been shown that the apparent rate constant of the *trans-cis* photoisomerisation in a relatively viscous media, for instance, in biological membranes, is controlled by the medium relaxation rate [6]. This method was also applied to studies of the microviscosity effects on the *trans-cis* photoisomerisation of the stilbene molecules immobilized onto quartz plates coated with lysozyme [7, 8]. The apparent *trans-cis* photoisomerisation rate constant of the process was found to be 3–4 times lower for the immobilised stilbene molecule than for the same free molecule in solution. That indicated that the surface and the protein sterically hindered the twisting motion of the stilbene molecule in the excited state.

The latest studies on molecular dynamics of an antibody binding site by using the above fluorescence-photochrome method led to development of the novel fluorochrome immunoassay (FCIA), which is based on the conjugation of a particular *trans*-stilbene derivative to an antibody of interest [9, 10]. This *trans*-stilbene derivative, which is a photochrome probe and analogue (hapten) to the native antigen of a

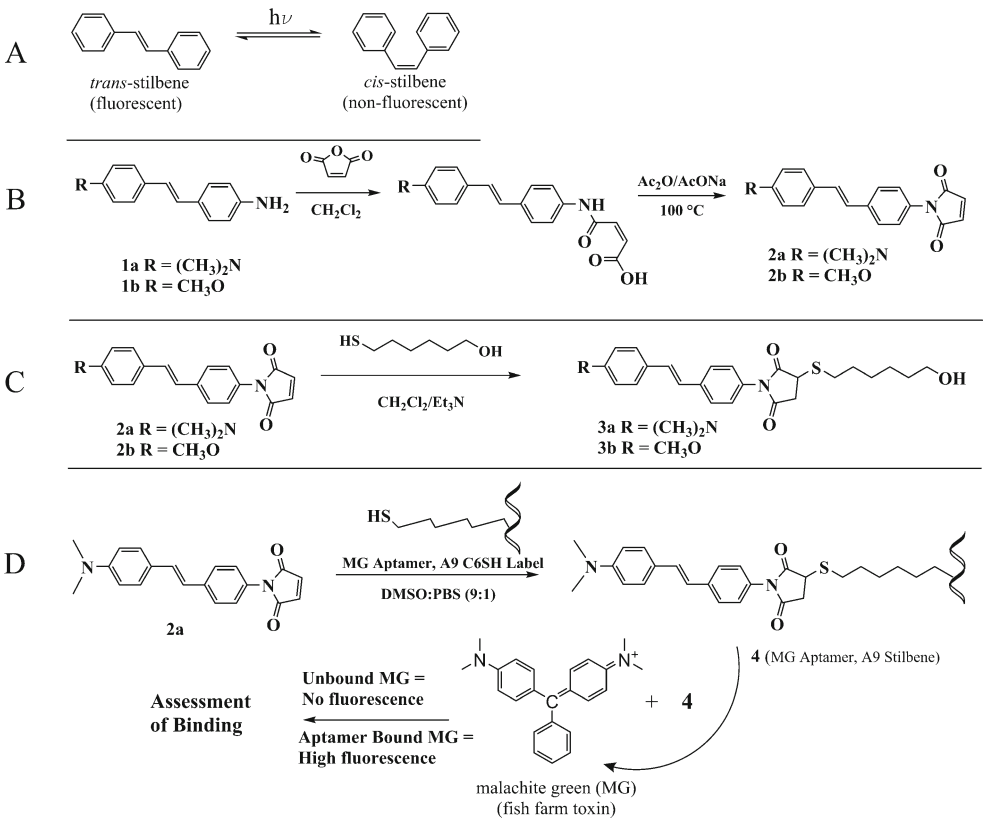

Fig. 1 Stilbene fluorescent switch. **a** Stilbene exists in two molecular configurations; the fluorescent trans-isomer is switched to the non-fluorescent cis-isomer upon irradiation at the excitation maximum. **b** Synthesis of stilbene-maleimides and their reaction with **c**) 6-mercaptohexanol yielding the conjugates 3a and 3b, and **d** Malachite Green (MG) Aptamer, A9 C6SH label yielding the conjugate **4**, MG Aptamer, A9 Stilbene

particular antibody, was completely prevented from the twisting motion upon irradiation with the excitation light within the antibody binding site. As a result, no change in fluorescence intensity of the *trans*-stilbene molecule was observed, and that was reported as almost zero fluorescence intensity decay with time compared to that of the free *trans*-stilbene molecule measured in solution [10].

The majority of commonly employed non-radioactive and non-enzyme immunoassays are based on physical labelling. The principle of biophysical labelling approach is based on chemical modification of chosen sites of the object of interest by special compounds (labels and probes) whose properties make it possible to trace the state of the biological matrix by appropriate physical methods. Several types of physical labelling immunoassays have been commonly used at present, such as Free-Radical Assay Techniques (FRAT); Liposome Immune Lysis Assay in a combination with FRAT (LILA-FRAT); Fluorescence Polarisation Immunoassay (FPIA); Fluorescence Resonance Transfer Immunoassay (FRTIA) and LILA Fluorescence Immunoassay (LILA-FIA). The general advantage of all these modern physical labelling immunoassays is monitoring the complex formation between antigens and antibodies in solution without preliminary separation. Each method has however its limitations. FRAT being monitored by ESR techniques requires relatively high concentration of the tested compound. Direct luminescence methods, such as FPIA and FRTIA, appear to be more sensitive but they require solutions of low optical density and cannot be used in biological or non-transparent media. FRAT and FPIA are not practically applicable to antigens of higher molecular weight. FRTIA requires preliminary labelling of both antigen and antibody and its limited by a molecular distance critical for the resonance energy transfer. LILA-FRAT and LILA-FIA, involve a complicated procedure of liposome preparation and loading with spin and fluorescent probes, and bearing covalently bound antibodies. The most commonly employed immunoassay methods for small antigen molecules appear to be the FPIA and FRTIA. However, they have two main disadvantages: they require special polarisation or resonance instruments, and they are insufficiently sensitive for incident and emitted light to be polarised. Also, the practical sensitivity of these methods does not make them commercially viable.

Being a non-separation and rapid immunoassay producing results within a few minutes and based on time-dependent fluorescence emission in-situ, the FCIA seems to have a number of essential advantages over all the above techniques. Also, the FCIA is a quantitative method and can measure the concentration of an analyte in a sample by a competitive binding of the analyte molecules to the active site of the antibodies occupied by the *trans*-stilbene-conjugates. Nevertheless, with all its advantages over the listed above techniques, it is still an antibody-based immunoassay with many disadvantages of using antibodies, which make it commercially non-applicable. Antibodies, although employed in many biosensor technologies today, have many essential drawbacks: 1) limited shelf-lives in the dry or hydrated state, 2) denature in organic solvents and aqueous mixtures, 3) display background fluorescence signals that lower signal-to-noise ratios, 4) tend to have bulky molecular volumes several orders of magnitude larger than the binding ligand of interest, thereby limiting high density and high intensity fluorescence measurements, 5) frequently fail to produce avid antibodies to hapten sized analytes such as TNT, and 6) the cross-reactivity for these small size targets is very high, leading to a lower specificity. Thus, due to their relatively big size, it is difficult for antibodies to recognize small molecules with high sensitivity and selectivity. Besides, antibodies suffer from batch to batch variation in their structure and functionality and denaturation and their generation process involves the use of animals. As a result, any bioassay or biosensing system based on the FCIA for detection of a certain analyte would differ in its sensitivity, and might be difficult to calibrate and make generic.

The aforementioned limitations of antibodies can be easily overcome by replacing them with aptamers, which are single strand DNA or RNA oligonucleotides. Aptamers are different from antibodies, yet they mimic properties of antibodies in a variety of diagnostic formats. They are attracting more and more attention as a replacement for antibodies due to their ease of manufacturing, strong affinity and excellent specificity even for small molecular weight targets. The main advantage of aptamers is their in-vitro selection process. By isolating aptamers in-vitro, an aptamer can be produced for any target molecule. Moreover, aptamers have very long shelf lives, can be rapidly screened by the SELEX method for new designs, and can be rapidly scaled for manufacturing. Aptamers are relatively small in size, can be stabilised in organic/aqueous solvents, and achieve high ligand-specificity. Therefore, they are a more logical choice for bioassays than antibodies, including the fact that higher surface densities can be placed in a microtiter plate well-the higher the density, the greater the sensitivity, especially when combined with metal enhanced fluorescence. Thus, due to their small size, tuneable stability, and high ligand-specificity, aptamers seem to be a more logical choice than antibodies in our proposed assay, as it will be described below.

Thus, for the first time, we report here the experimental studies connected to development of the novel photochrome-aptamer switch assay (PHASA) allowing state-of-the-art analyte detection and quantification of small molecules such as toxins, explosives, drugs and pollutants, which are difficult to detect using antibodies-based assays with high sensitivity and specificity, in minutes. In the first stage of the PHASA development, we have focused on the so called “adaptive binding” of the stilbene compound to an aptamer of interest, as it will be explained in the next section. Synthetic preparation and

experimental studies of the novel stilbene-maleimide switches and their adaptive binding to the thiolated Malachite Green aptamer are described in the present manuscript.

Experimental

Reactants and Solvents

Reactants were either commercially available or freshly prepared as detailed in the "Synthesis" section. Commercially available organic solvents, namely dimethyl sulfoxide (Sigma-Aldrich ACS spectrophotometric grade, ≥99 %) and ethanol (Sigma-Aldrich ACS spectrophotometric grade, ≥99 %), used for spectroscopy did not require any additional purification.

Apparatus and Methods

Semi-preparative flash chromatography used for purification of the compounds was performed with the Büchi Sepacore® flash chromatography system using 25 g silica gel cartridges (particle size 40–63 μm) and dichloromethane as an eluting solvent. ^{1}H NMR spectra were run on 10 % (w/v) sample solutions in $CDCl_3$ with $(CH_3)_4Si$ as an internal standard at room temperature using a 400 MHz Bruker Fourier transform spectrometer, equipped with a DMX AVANCE I system. UV absorption spectra were measured using an Agilent Cary 300 spectrophotometer, and the steady-state fluorescence spectra were recorded with Horiba Jobin Yvon FluoroLog®-3 modular spectrofluorometer and Agilent Cary Eclipse fluorescence spectrophotometer. The fluorescence excitation and emission spectra were corrected for instrumental sensitivity at different excitation and emission slits using the instrument internal excitation-emission matrix (EEM) correction [11, 12]. A solution of quinine bisulphate in 0.1 N H_2SO_4 (Φ_f=0.52) was taken as fluorescence standard for the determination of fluorescence quantum yields [13]. Constant-illumination fluorescence intensity decay curves at the photostationary steady-state equilibrium between the *trans*- and *cis*-isomers of stilbenes were recorded with Shimadzu RF-5301 spectrofluorometer equipped with the 150 W Xenon lamp as a radiation light source. The fluorescence decay at the photostationary steady-state equilibrium was monitored at the emission maximum of the stilbenes after excitation at the excitation maximum using typically 5-nm slit width for excitation and 5-nm slit width for emission. Analysis of the experimental data was performed using Origin® Pro 9.0 for Windows. Fluorescence intensity decay curves were analysed with a polynomial fit for calculation of the *trans-cis* isomerization rate constants using a self-written routine within the Origin® Pro 9.0 for analysis of the first-order photochemical reaction rates. Mass spectroscopy analysis was performed on a Shimadzu Biotech Axima TOF^2 in linear positive mode and calibrated against lysozyme (m/z 14306). Samples were spotted *neat* or with 2,4,6-trihydroxyacetophenone (10 mg in 250 μL ACN).

Synthesis

The following reactants were prepared by slight modification of our procedure that we published in [6]: *trans*-4-*N,N′*-dimethylamino-4′-nitrostilbene, *trans*-4-methoxy-4′-nitrostilbene, *trans*-4-*N,N′*-dimethylamino-4′-*N*-aminostilbene and *trans*-4-methoxy-4′-*N*-aminostilbene.

Trans-4-N,N'-Dimethylamino-4'-Nitrostilbene (DANS)

An equimolar mixture of 4-nitrophenylacetic acid (Sigma-Aldrich N20204) (9.1 g) and 4-(dimethylamino)benzaldehyde (Sigma-Aldrich 156477) (7.5 g) in 3 mL of piperidine was heated for 24 h under reflux in an oil bath maintained at 140°. The resulting dark-red crude solid was recrystallized from 100 mL of chlorobenzene. Upon cooling, the product precipitated as lustrous red flakes, then was collected by vacuum filtration on a Buchner funnel, thoroughly washed with petroleum ether (60–80°) to remove the adherent piperidine and dried in a vacuum oven at 60° for about 2 h. Yield of the lustrous red flakes—7.4 g (53 %). Chemical purity and structural identity of the product was confirmed by ^{1}H NMR.

4-Nitrobenzyltriphenylphosphonium Bromide

Triphenylphosphonium salt was prepared from the corresponding 4-nitrobenzyl bromide (Sigma-Aldrich N13054) and triphenylphosphine (Fluka 93090) in toluene by slight modification of Wittig reaction [14]. In short, 2.16 g (10 mmol) of 4-nitrobenzyl bromide and 3.14 g (12 mmol) of triphenylphosphine were dissolved in 50 mL of toluene, and the reaction mixture was heated and stirred at 70 °C overnight. The precipitated salt was collected by vacuum filtration on a Buchner funnel and washed twice with acetone and petroleum ether and then dried in a vacuum oven at 80 °C for two hours. Yield of the crystalline white powder—4.58 g (96 %). It was used in the next step without further purification.

Trans-4-Methoxy-4'-Nitrostilbene

4.58 g (9.6 mmol) of the prepared 4-nitrobenzyltriphenylphosphonium salt and 1.50 g (11 mmol) of *p*-anisaldehyde (Sigma-Aldrich A88107) were dissolved in 25 mL of absolute methanol. 25 mL of 0.4-M lithium methoxide solution in absolute methanol was added, and the dark red reaction mixture was intensively stirred at room temperature for 20 min. The resulting solution was left to stand overnight at room temperature to provide the

precipitation of the product. The precipitated orange crystals of the *trans*-isomer were collected by vacuum filtration on a Buchner funnel and re-crystallised from ethanol. Yield of the bright orange crystals—1.77 g (72 %). ^{1}H NMR (chemical shifts are in ppm): δ 3.85 (singlet, 3H, MeO); CH=CH AB pattern: δ 6.98 (doublet, vinyl 1H), δ 7.23 (doublet, vinyl 1H); *p*-MeO-Ar AA'XX' pattern: δ 6.98 (doublet, 2H: H3, H5), δ 7.49 (doublet, 2H: H2, H6); *p*-O_2N-Ar AA'XX' pattern: δ 7.59 (doublet, 2H: H2′, H6′), δ 8.20 (doublet, 2H: H3′, H5′). Melting point of 150–151 °C was found to be in a good agreement with the literature value [14].

*Trans-4-N,N′-Dimethylamino-4′-N-Aminostilbene (**1a**, Fig. 1b)*

Solution of 120 g of potassium hydroxide pellets dissolved in 200 mL of ultrapure water was prepared in 500 mL Erlenmeyer flask and placed in a fridge for storing. This solution is used for decomposition of the prepared stannous complex salt of the product. 15 g of stannous chloride dihydrate was dissolved in 150 mL of concentrated hydrochloric acid at room temperature with stirring. 4 g of fresh *trans*-4-dimethylamino-4′-nitrostilbene prepared in the previous step was introduced into the stirred solution of $SnCl_2$. The suspension was refluxed for about 4–5 h until all red flakes and orange viscous particles of the intermediate stannous complex salt formed during the reaction have been completely dissolved, and the yellow reaction mixture has become transparent. The reaction mixture was stirred for additional half an hour and allowed to cool to the point of turbidity. Then it was poured carefully into a cold stirred solution of potassium hydroxide taken from the fridge and placed into an ice bath, in order to decompose the complex stannous salt and to release the product. Caution: the neutralization reaction is highly exothermic and vigour! Well-protective glasses, gloves and clothes should be worn during this step, and all precautions for minimising the reaction mixture splashing should be taken. The crude yellow product was collected by vacuum filtration, thoroughly washed with 10 % sodium bicarbonate solution, ultrapure water and then with petroleum ether (60–80°). The crude yellow product was dissolved in 10 mL of dichloromethane, and subjected to the flash chromatography on the regular silica gel (particle size 40–63 μm). The fractions containing *trans*-isomer (λ_{abs}=360 nm) were collected and evaporated to yield the yellow amorphous powder (2.82 g, 77 % reaction yield). Chemical purity was >99 % as determined by RP-HPLC and structural identity of the product was confirmed by ^{1}H NMR, 400 MHz, CDCl3: 7.41–7.38 (2H; d; 8.78Hz); 7.33–7.31 (2H; d; 8.46 Hz); 6.92–6.88 (1H; d; 16.36 Hz) 6.87–6.83 (1H; d; 16.36 Hz); 6.75–6.72 (2H; d; 8.78 Hz); 6.70–6.68 (2H; d; 8.40 Hz); 3.71 (broad s; 2H); 2.99 (s; 6H).

*Trans-4-Methoxy-4′-N-Aminostilbene (**1b**, Fig. 1b)*

Trans-4-methoxy-4′-nitrostilbene was reduced in a similar manner as DANS with stannous chloride dihydrate in concentrated hydrochloric acid to afford the corresponding aminostilbene. The product was purified with the flash chromatography on the silica gel (particle size 40–63 μm) with dichloromethane as an eluent solvent. The fractions containing *trans*-isomer (λ_{abs}=330 nm) were collected and evaporated to yield the white amorphous powder, which was recrystallised from ethanol to yield white small needles with the 63 % reaction yield. Sample of the product was submitted for ^{1}H NMR, 400 MHz, CDCl3:: 7.60–7.58 (2H; d; 8.53 Hz); 7.50–7.48 (2H; d; 8.72 Hz); 7.36–7.34 (2H; d; 8.46 Hz); 7.12–7.08 (1H; d; 16.23 Hz); 7.02–6.98 (1H; d; 16.29 Hz); 6.94–6.92 (2H; d; 8.65 Hz); 6.88 (2H; s); 3.86 (3H; s).

*Trans-4-N,N′-Dimethylamino-4′-Stilbene Maleimide (**2a**)*

Step1: Preparation of the maleamic acid intermediate.

Stilbene-maleimides and the corresponding sulphides were prepared according to the reaction scheme seen in Fig. 1b and c. Maleic anhydride (0.98 g, 10 mmol, Fluka 63200) and 50 mL of DCM were introduced into a round-bottom flask equipped with a condenser and a heated magnetic stirrer. After maleic anhydride dissolution, **1a** (1.9 g, 8 mmol) was added and the mixture stirred at RT for 1.5 h to complete the reaction whereby the crude dark red product was precipitated and collected by vacuum filtration after cooling in an ice bath. The product was washed with deionized water, DCM, and vacuum dried. If desired, the intermediate maleamic acid may be recrystallized from DMF or DMF/water mixture.

Step 2: Preparation of the maleimide (**2a**).

The maleamic acid from the previous step was cyclised by dehydration with acetic anhydride and sodium acetate as described in the literature [15, 16]. Briefly, 7 mmol of the obtained maleamic acid was mixed with 0.35 g of anhydrous sodium acetate and 10 mL of acetic anhydride. Upon stirring and heating at 100 °C, the suspension was dissolved and the resulting solution gradually changed colour from dark red to dark yellow. After 45 min of heating the reaction mixture was allowed to cool for 1 h and poured on ice. Stirring the ice mixture for 30 m (until the ice melted) resulted in a separation of a dark red precipitate, which was collected by vacuum filtration, washed with ultrapure water and vacuum dried. The product was purified with the flash chromatography on the silica gel (particle size 40–63 μm) with DCM eluent. Yield of the purified maleimide is 71 % and purity is >99 % as assessed by RP-HPLC. ^{1}H-NMR, 400 MHz, DMSO-d6:

7.64–7.62 (2H; d; 8.53 Hz); 7.47–7.44 (2H; d; 8.84 Hz); 7.30–7.28 (2H; d; 8.53 Hz); 7.19 (2H; s); 7.20–7.16 (1H; d; 16.29 Hz); 7.03–6.99 (1H; d; 16.42 Hz); 6.75–6.72 (2H, d, 8.91 Hz); 2.95 (6H; s).13C-NMR, DMSO-d6: 170.44; 150.58; 137.85; 135.16; 130.17; 130.12; 128.14; 127.32; 126.50; 125.17; 123.03; 112.67. MALDI TOF (*neat*; reflectron mode, positive) e/z 318.15 [M]+ (calculated 318.14).

*Trans-4-Methoxy-4'-Stilbene Maleimide (***2b***)*

2b was prepared in a similar manner as **2a** in two steps starting from **1b** and maleic anhydride and further cyclising the obtained corresponding maleamic acid by dehydration with acetic anhydride and sodium acetate. After purification with the flash chromatography, light lemon-yellow crystals were obtained. Purity is >99 % as assessed by RP-HPLC. ^{1}H-NMR, 400 MHz, DMSO-d6: 7.60–7.58 (2H; d; 8.53 Hz); 7.50–7.48 (2H; d; 8.72 Hz); 7.36–7.34 (2H; d; 8.46 Hz); 7.12–7.08 (1H; d; 16.23 Hz); 7.02–6.98 (1H; d; 16.29 Hz); 6.94–6.92 (2H; d; 8.65 Hz); 6.88 (2H; s); 3.86 (3H; s). ^{13}C-NMR, DMSO-d6, 170.40; 159.60; 137.32; 135.19; 130.72; 129.96; 129.43; 128.40; 127.33; 126.88; 125.65; 114.68; 55.65. MALDI TOF (*neat*, reflectron mode, positive) e/z 306.13 [M+H]+ (calculated 306.11).

Reaction of **2a/b** *with 6-Mercaptohexanol towards* **3a/b** *(Fig. 1c)*

Either 2a or 2b (0.272 mmol) was dissolved in 4 mL of dichloromethane. Isopropanol and triethylamine (0.4 mL each) were added followed by addition of 6-mercaptohexanol (70 μL, 0.51 mmol). The mixture was stirred for 4 h to complete the reaction, the progress of which was monitored with silica-TLC. The reaction mixture was then evaporated and the remaining white residue was washed with isopropanol, methanol and vacuum dried. Reaction yields of approximately 75 % were obtained. **3b**, ^{1}H-NMR, 400 MHz, DMSO-d6: 7.69–7.67 (2H; d; 8.46 Hz); 7.59–7.56 (2H; d; 8.78 Hz); 7.29–7.25 (1H; d; 16.67 Hz); 7.26–7.24 (2H; d; 8.46 Hz); 7.17–7.13 (1H; d; 16.48 Hz); 6.98–6.96 (2H; d; 8.78 Hz); 4/37–4.34 (1H; t; 5.15 Hz; −O**H**); 4.13–4.09 (1H; dd; 9.12 Hz; 4.14 Hz); 3.79 (3H; s); 3.41–3.38 (2H; t; 6.25 Hz); 2.86–2.74 (2H; m); 2.72–2.67 (1H; dd; 18.31 Hz; 4.10 Hz); 1.65–1.53 (2H; m); 1.46–1.28 (6H; m). ^{13}C-NMR, DMSO-d6, 176.42; 174.78; 159.65; 138.03; 131.36; 129.91; 129.72; 128.45; 127.56; 126.92; 125.57; 114.69; 61.09; 55.65; 36.67; 36.67; 32.86; 31.02; 29.18; 28.56; 25.53. MALDI-TOF (*neat*; reflectron mode, positive) m/z 440.46 [M+H]+ (calculated 440.19).

Reaction of **2a** *with thiolated MG Aptamer, A9 C6SH Label to Yield* **4***, MG Aptamer, A9 Stilbene conjugate (Fig. 1d)*

MG RNA aptamer (NCBI Accession:1Q8N_A) A9 modified with C6SH label (5 nmol, AITbiotech, Singapore) as solution in 40 μL of PBS buffer was treated with TCEP (1 μL; 40 mM solution in PBS buffer) to activate its thiol group during 30 min at r.t. Then 340 μL DMSO and 24 μL of 4′-dimethylamino-stilbenyl-4-maleinimide stock solution in DMSO (8.67 mM, i.e. 208 nanomoles of the maleimide) were added. Vortexing resulted in clear solution, which was left at room temperature overnight. RNA was precipitated with 90 μL 5 M aqueous ammonium acetate and 1.7 mL isopropanol. Upon keeping at −20 °C and centrifugation (13,000 rpm; 30 min) an RNA pellet was formed. The supernatant was removed and the remaining pellet was washed with isopropanol (3×1 mL). Then the pellet was re-dissolved in 600 uL of PBS buffer. OD (260 nm) 0.579; calculated concentration 1.226 μM. Thus 0.735 nanomoles of the conjugated aptamer was obtained and the yield was 14 %. According to RP-HPLC there was no starting maleimide detected and the purity was assessed >99 %. MALDI-TOF. Theoretical m/z (12514, $[M+H]^{+}$); Supplier m/z: A9 modified with C6SH label, **12515**, $[M+H]^{+}$; Shimadzu MALDI-TOF (THAP matrix, reflection mode, positive), A9 modified with C6SH label, 12615, $[M+H+DMSO+H2O]^{+}$, Shimadzu MALDI-TOF (THAP matrix, reflectron mode, positive), **4**, 12833, $[M+H]^{+}$.

Results and Discussion

The PHASA bioassay is based on the conjugation of a switchable *trans*-stilbene molecule to any aptamer of interest and utilizes the numerous advantages of aptamers, such as their high binding affinity and specificity, stability and easy chemical synthesis. The mechanism of operation behind PHASA relies on the *trans-cis* photoisomerisation of a stilbene-ligand compound having a chemical moiety (ligand) matching the analyte of interest. As mentioned above, the *trans-cis* photoisomerisation rate of the stilbene compound is depended on the surrounding media, which can be used to indicate the presence of the analyte and its further quantification. Quantification of the PHASA is essentially based on the constant-illumination fluorescence decay of the *trans*-isomer toward the photostationary equilibrium that removes cumbersome and error-prone light intensity calibrations. The signal is monitored under constant-illumination conditions as a time trace or gradient of the fluorescence emission decay.

We have recently developed two formats of the PHASA: competitive and adaptive binding formats. The competitive binding format will be briefly reviewed below and is a subject of the subsequent publication, while the experimental studies

related to the adaptive binding format will be described in the present manuscript.

Competitive Binding

The method for analyte detection and concentration measurement in a sample based on a direct conjugation between the stilbene-ligand molecule and the analyte-specific aptamer involves a competitive binding of the free analyte molecules present in the sample to the binding site of the aptamer. This will competitively replace the stilbene-ligand molecule initially forming a complex with the analyte-specific aptamer as shown in Fig. 2. Introduction of a sample containing the analyte, results in a competitive analyte-aptamer complex formation. This subsequently releases the fluorescent *trans*-stilbene-ligand molecule from the aptamer into solution that is observed as a significant acceleration of the fluorescence decay of the *trans*-isomer upon irradiation with the excitation light. Analyte concentration is calibrated to the *trans-cis* photoisomerisation rate constant to provide a quantification of the assay.

Adaptive Binding

Besides the above competitive binding format, direct covalent attachment of the stilbene probe with the modified aptamer followed by adaptive binding of the analyte molecules can also lead to the generation of a calibration curve for practical applications. Thus, the following mechanism has been put forward, by making use of the adaptive binding property of aptamers. This refers to the aptamer changing its folding and shape after binding to the analyte. In this case, instead of using the stilbene-ligand molecule, the stilbene molecule can be directly covalently attached to the aptamer via a crosslinker. The mechanism works by allowing the aptamer to fold or unfold around the attached stilbene molecule and can be classified into two cases:

In **Case 1**, following the covalent binding of the stilbene onto an aptamer, the adaptive binding of the aptamer is induced resulting in the stilbene being squeezed inside the aptamer, and its fluorescence decay becomes slow. This situation is shown in Fig. 3a. In **Case 2**, following the covalent binding of the stilbene molecule onto an aptamer, the aptamer folds around the stilbene, sterically hindering the twisting motion of the stilbene molecule in the excited state, resulting in relatively slow fluorescence decay. When the analyte B is added, the aptamer folds around the analyte, exposing the stilbene to solution and thus, the fluorescence decay becomes fast. This can be illustrated in Fig. 3b.

The crosslinker that we used in our studies of the adaptive binding format is maleimide, where 'click chemistry' allows for efficient covalent binding of the stilbene to the aptamer. The stilbene-maleimide was attached directly to the thiol-modified aptamer by the click-like chemistry as shown in Fig. 1d.

The prepared maleimides **2a** and **2b** were fully characterised. Figure 4a, b, and c displays the absorption, fluorescence excitation and emission spectrum of the stilbene-maleimides, respectively. Their fluorescence decay kinetics to the photostationary state under constant-illumination conditions is shown in Fig. 4d. There is a strong red-shift of the absorption and fluorescence emission maximum observed

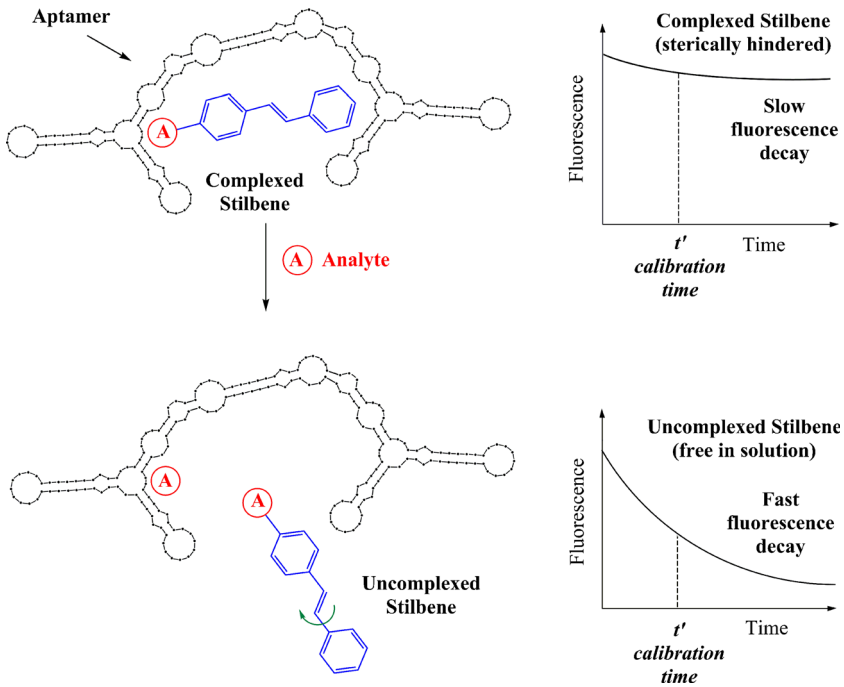

Fig. 2 PHASA competitive binding format illustrated with the detection and quantification of Analyte A. The stilbene-ligand switch is initially bound to the analyte-specific aptamer. Free analyte replaces a portion of the stilbene-ligand conjugates. The fluorescence decay rate is then measured and calibrated to the free analyte concentration

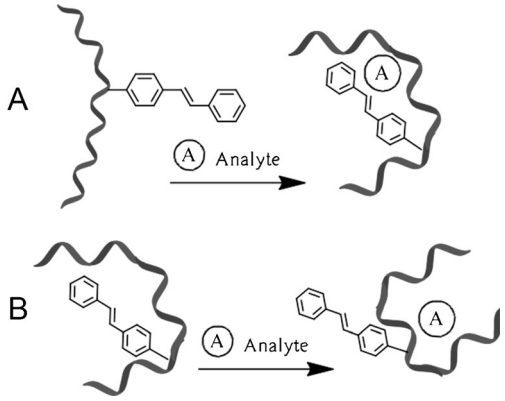

Fig. 3 **a** Case 1 where the adaptive binding of the analyte A results in retardation of the fluorescence decay. **b** Case 2 where the adaptive binding of the analyte A results in acceleration of the fluorescence decay

in the spectra of **2a** compared to **2b**, and can be explained by the presence of the strong donor dimethylamino (DMA) group substituent at the *para*-position of the aromatic ring. The DMA group facilitates the charge delocalization in the ground state ^{1}t of **2a** that results in a lower energy and longer wavelength transition to the Frank-Condon state [3, 2]. It also stabilizes the excited ^{1}t* state of **2a** in comparison with **2b**, thereby increasing the Stock shift. The spectral properties of the measured compounds are summarised in Table 1, which brings together the absorption (λ_{abs}), fluorescence excitation and emission (λ_{ex} and λ_{em}) maxima, fluorescence quantum yields (Φ_f) and apparent *trans-cis* photoisomerisation rate constants (K_{app}) for the investigated compounds

The measured fluorescence quantum yield **2b** is almost twice as low compared to the stilbene-maleimide-MCH adduct **3b**. We assume that part of the additional non-radiative losses in **2b** are caused by the electronic energy transfer onto the maleimide acceptor fragment, which intrinsically shows negligible fluorescence, due to the presence of an efficient conical intersection of the S_1 state with the ground state S_0 [17]. The effect should be even more pronounced in **2a** having the lowest quantum yield, since the DMA group is a stronger electronic donor than methoxy group. Drastic increase of the quantum yield of **3b** then should be connected to the destruction of the charge transfer interaction between the donor methoxy and maleimide acceptor substituents, as a result of the chemical reaction with MCH that removes the conjugation/electronic delocalization in the maleimide ring and thereby decreases its acceptor power.

It is known that the *trans-cis* photoisomerisation process of stilbene compounds can be sterically hindered by their surrounding environment [7, 8]. Medium viscosity effects on the *trans-cis* photoisomerisation of both stilbene-maleimides are shown in Fig. 5a and b. In order to study the medium viscosity effect on the fluorescence decay rate of **2a**, **2b** and **3b** (Fig. 5a–c), several aqueous glycerol solutions of the compounds having the same concentration were prepared. Viscosity of these solutions was varied by adding in different amounts of glycerol and measured using the Brookfield viscometer. The fluorescence decays were measured and the corresponding *trans-cis* photoisomerisation rate constants were calculated. The logarithmic dependence of the *trans-cis*

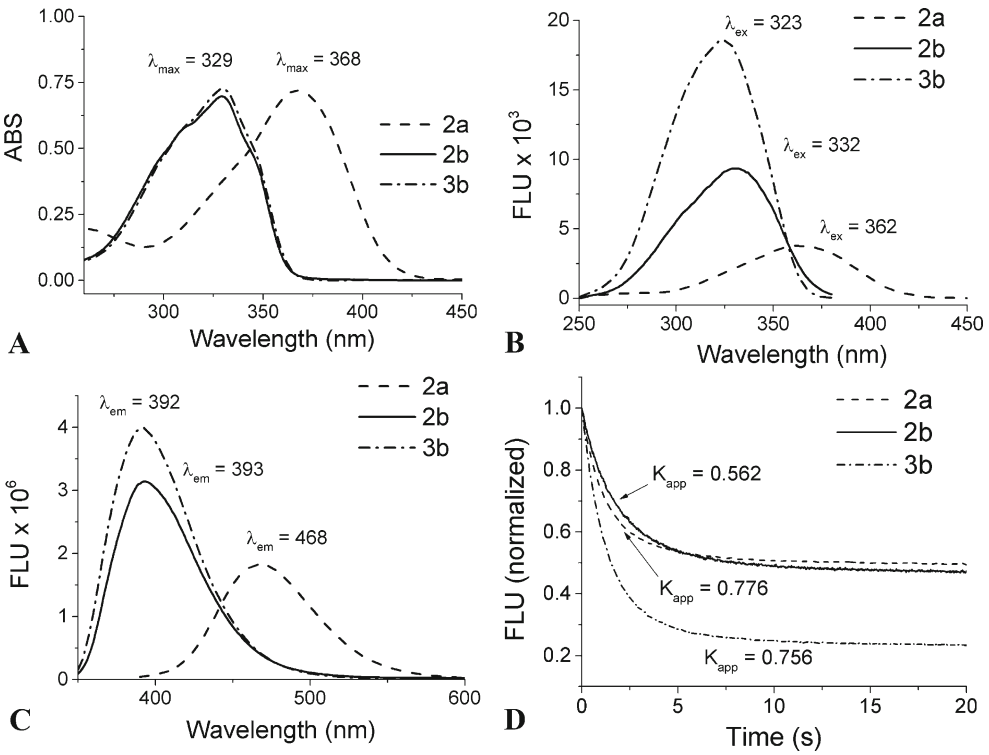

Fig. 4 **a** Absorption spectrum of 2a, 2b, and 3b in DMSO (20 μM for all, **b** Fluorescence excitation spectrum of 2a, 2b, and 3b in DMSO (2 μM for all), **c** Fluorescence emission spectrum in DMSO (2 μM for all) and **d** Fluorescence decay kinetics in DMSO (2 μM for all)

Table 1 Absorption (λ_{abs}), fluorescence excitation and emission (λ_{ex} and λ_{em}) maxima, fluorescence quantum yields (Φ_f) and apparent trans-cis photoisomerisation rate constants (K_{app}) for **2a**, **2b** and **3b**

	λ_{max} (nm)	λ_{ex} (nm)	λ_{em} (nm)	Quantum yield	Apparent *trans-cis* photoisomerisation rate constant (s^{-1})
2a	368	362	468	0.009±0.001	0.776
2b	329	332	393	0.015±0.001	0.562
3b	329	323	392	0.032±0.001	0.756

photoisomerisation rate constant on the reciprocal medium viscosity is shown in Fig. 5d.

From Fig. 5d, it can be observed that for all the three compounds, certain linear detection range exists. For **2a**, the equation for analyte quantification in the linear detection range (solid line) can be described by $K_{app}=(1.066\pm0.011)+(0.309\pm0.012)\ \log\ (1/\eta)$. For **2b**, it is described by $K_{app}=(0.726\pm0.009)+(0.083\pm0.005)\ \log\ (1/\eta)$ and $K_{app}=(0.824\pm0.009)+(0.098\pm0.005)\ \log\ (1/\eta)$ for the **3b**.

In view of the above results, we can conclude that the fluorescence decay rate is indeed strongly dependent on medium viscosity. With increase of the medium viscosity, retardation of the fluorescence decay is clearly observed, which can be considered as an indicator of the steric freedom for the twisted motion of the stilbene molecule in the excited state within its lifetime. In other words, the change of fluorescence decay rate constant with medium viscosity confirms that there is a strong dependence of the *trans- cis* photoisomerisation process on the viscosity of the surrounding medium. The logarithmic curve shown in Fig. 5d makes it possible to quantify the method and establish the sensitivity range of the stilbene switches.

Malachite Green Aptamer Conjugation to Stilbene (4) Retains Malachite Green Binding Ability

Malachite green (MG)-aptamer, a 38 nt single-stranded RNA (NCBI #1Q8N), was synthesized by solid-phase synthesis from a local supplier and was found to have a K_d of 800± 200 nM, which is in agreement with that reported in the literature [18–20]. Four sites of nucleotide C6SH (thiol) modification (U4, A9, C20, and C38) were chosen based on their non-essential nature, distance from the binding pocket and surface exposure to the solvent [18, 20]. The A9 C6SH modification was found to have the lowest binding affinity of 700±100 nM to MG, although all 4 nucleotide C6SH modifications had binding affinities below 1,000 nM. The MG aptamer A9 C6SH label was chosen for grafting by **2a**–**2a** happens to be slightly more soluble than **2b**. Grafting of **2a** to MG aptamer A9 C6SH label was accomplished by reacting

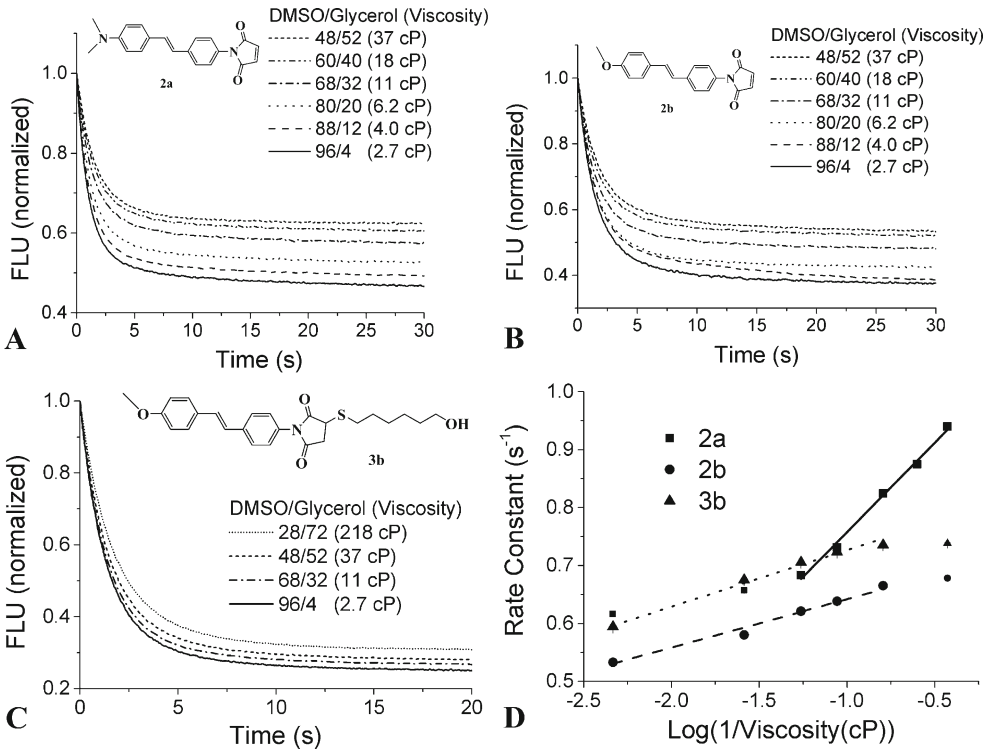

Fig. 5 Viscosity profile of 2 μM **a** 2a **b** 2b and **c** 3b. **d** The logarithmic dependence of the trans-cis photoisomerization rate constant on the reciprocal medium viscosity for 1 μM of 2a, 2b, and 3b

in DMSO/10 % PBS and precipitation of **4** in isopropanol as depicted in Fig. 1d. Reverse phase-HPLC found equal molar amounts of MG aptamer (ABS @ 260 nm) and the **2a** (ABS @ 340) eluting at the same peak times, with no traces of unbound **2a** as seen in Fig. 6a and b. Binding affinity of the MG to **4** was subsequently assessed by following the fluorescence of MG. When MG is bound within the MG-aptamer pocket, it exhibits a quantum yield three orders of magnitude higher than unbound MG due to planarization of the molecule as a result of the electron delocalization in its excited state [21, 22]. We can take advantages of this unique feature for easy assessment of binding coefficients, which can be calculated by ubiquitous fluorescent microplate readers. Figure 6c displays the fluorescence emission of **4**, MG, and **4** + MG—little to no fluorescence is seen for **4** or free MG. However when mixed, a high fluorescence intensity signal was seen, indicating that the **4** MG Aptamer, A9 stilbene retained its ability to bind to MG with affinity similar to the wild-type MG aptamer and unconjugated MG aptamer A9 C6SH label. This shows that in the presence of the bound stilbene molecule, the MG successfully enters the binding pocket of the aptamer, which substantiates the mechanism of adaptive binding format described above. Due to manuscript constraints, our subsequent publication will further investigate the adaptive binding photodecay kinetics and analyte sensitivity of MG Aptamer modified with stilbene at the four positions previously mentioned: U4, A9, C20, and C38.

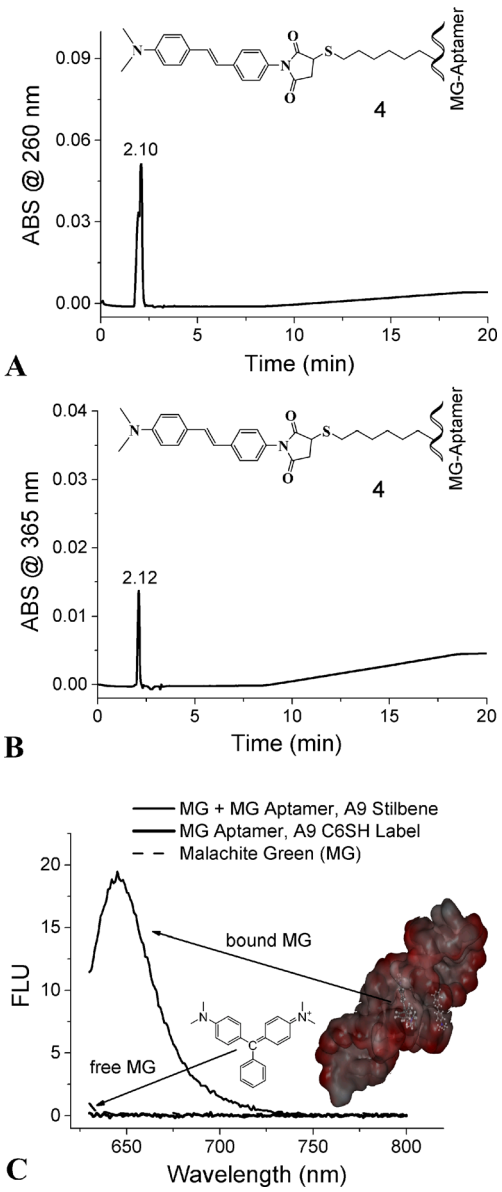

Fig. 6 RP-HPLC characterization of **4** by two ABS wavelengths of **a** 260 nm, which allows quantitation of the MG-aptamer and **b** 365 nm, which allows quantitation of **2a. c** Fluorescence intensity of free MG, **4**, bound MG with the MG-aptamer binding pocket of **4**

Conclusions

Aptamers existing on the market are available for over 150 targets, mostly for therapeutic purposes. This leaves much opportunity for PHASA to be quickly developed towards numerous applications. Should a particular aptamer be unavailable, it can be easily designed and manufactured in 6–8 weeks for a reasonable cost, which would be unfeasible (if not impossible) for antibodies. Aptamers will allow for more novel designs and continued development of the next generation PHASA biosensors. A key design feature in the PHASA platform is based on the 'no-separation-needed' concept—reagents and bound aptamers will require no discrete separation protocols or washing procedures before or after measurements. It is essentially a one-step procedure that is self-contained. The bioassay can operate not only in aqueous solutions but also in a solvent mixtures, heavily contaminated heterogeneous wastes and biological media collected in a single tube, without separate purification protocols. Eventually, the PHASA assay permits not only the instant detection of an analyte in a sample but also rapid (within a few minutes) determination of its concentration.

In the first stage of the PHASA development, we have focused on the adaptive binding of the stilbene compound to an aptamer of interest, as shown in Figs. 3 and 6. Synthetic preparation and experimental studies of the novel maleimide-stilbene compounds and their adaptive binding to the thiolated Malachite Green aptamer, **4**, are described in the present manuscript.

Acknowledgments The authors wish to thank Dr. Vitali Lipik for his invaluable help with the MALDI-TOF analysis of the samples. This research is funded by the Singapore National Research Foundation and the publication is supported under the Campus for Research Excellence and Technological Enterprise (CREATE) programme (13-04-00364 A). The authors thank Huang Ruo Cheng, Tan Chong Yuan and Terence Mak

of River Valley High School for their active participation in this project in the frame of the program for Singapore Science & Engineering Fair. In addition, the authors thank NTU for providing partial financial support to this program. Funding was also greatly appreciated from the Ministry of Education Tier 1 Grant: Photochrome aptamer switch assay: A universal bioassay device - RG54/13.

References

1. Görner H, Kuhn HJ (2007) Cis-trans photoisomerization of stilbenes and stilbene-like molecules. In: Advances in photochemistry. John Wiley & Sons, Inc, Hoboken, pp 1–117. doi:10.1002/9780470133507.ch1
2. Papper V, Likhtenshtein GI (2001) Substituted stilbenes: a new view on well-known systems: new applications in chemistry and biophysics. J Photochem Photobiol A Chem 140(1):39–52. doi:10.1016/S1010-6030(00)00428-7
3. Papper V, Pines D, Likhtenshtein G, Pines E (1997) Photophysical characterization of trans-4,4′-disubstituted stilbenes. J Photochem Photobiol A Chem 111(1–3):87–96. doi:10.1016/S1010-6030(97)00234-7
4. Waldeck DH (1991) Photoisomerization dynamics of stilbenes. Chem Rev 91(3):415–436. doi:10.1021/cr00003a007
5. Ahluwalia A, De Rossi D, Giusto G, Chen O, Papper V, Likhtenshtein GI (2002) A fluorescent-photochrome method for the quantitative characterization of solid phase antibody orientation. Anal Biochem 305(2):121–134. doi:10.1006/abio.2002.5601
6. Likhtenshtein GI, Bishara R, Papper V, Uzan B, Fishov I, Gill D, Parola AH (1996) Novel fluorescence-photochrome labeling method in the study of biomembrane dynamics. J Biochem Biophys Methods 33(2):117–133. doi:10.1016/S0165-022X(96)00022-X
7. Parkhomyuk-Ben Arye P, Strashnikova N, Likhtenshtein GI (2002) Stilbene photochrome-fluorescence-spin molecules: covalent immobilization on silica plate and applications as redox and viscosity probes. J Biochem Biophys Methods 51(1):1–15. doi:10.1016/S0165-022X(01)00234-2
8. Strashnikova N, Papper V, Parkhomyuk P, Likhtenshtein GI, Ratner V, Marks R (1999) Local medium effects in the photochemical behavior of substituted stilbenes immobilized on quartz surfaces. J Photochem Photobiol A Chem 122(2):133–142. doi:10.1016/S1010-6030(99)00009-X
9. Chen O, Glaser R, Likhtenshtein GI (2003) Molecular dynamics investigation of an antibody binding site by the fluorescence–photochrome method. Biophys Chem 103(2):139–156. doi:10.1016/S0301-4622(02)00252-1
10. Chen O, Glaser R, Likhtenshtein GI (2008) The novel FluoroChrome ImmunoAssay—(FCIA). The role of molecular environment upon molecular structure exemplified by constriction of a flourescence-photochrome flanked by two proteins. J Biochem Biophys Methods 70(6):1073–1079. doi:10.1016/j.jbbm.2007.07.007
11. Horiba Scientific, "NIST develops fluorescence standards with FluoroLog", Fluorescence Technical Note FL-30. (n.d.). http:www.horiba.com/fileadmin/uploads/Scientific/Documents/Fluorescence/FL-30_NIST_Fluorolog.pdf. Accessed 27 July 2014
12. Meir A, Stojanovic M, Marks RS (2007) Aptameric Biosensors. In: Marks RS, Cullen D, Lowe C, Weetall HH and Karube I (eds). Handbook of Biosensors and Biochips, John Wiley & Sons Ltd Publishers, Chapter 15, pp 217–232
13. Meech SR, Phillips D (1983) Photophysics of some common fluorescence standards. J Photochem 23(2):193–217. doi:10.1016/0047-2670(83)80061-6
14. Manecke G, Lüuttke S (1970) Über Synthesen einiger oligomerer substituierter Arylenvinylene. Chem Ber 103(3):700–707. doi:10.1002/cber.19701030308
15. Steele TWJ, Shier WT (2010) Dendrimeric alkylated polyethylenimine nano-carriers with acid-cleavable outer cationic shells mediate improved transfection efficiency without increasing toxicity. Pharm Res 27(4):683–698. doi:10.1007/s11095-010-0058-1
16. Cava MP, Deana AA, Muth K, Mitchell MJ (1961) N-Phenylmaleimide. Org Synth 41:93. doi:10.15227/orgsyn.041.0093
17. Braun D, Rettig W (1997) Excitation energy dependence of the kinetics of charge-transfer formation. Chem Phys Lett 268(1–2):110–116. doi:10.1016/S0009-2614(97)00156-5
18. Flinders J, DeFina SC, Brackett DM, Baugh C, Wilson C, Dieckmann T (2004) Recognition of planar and nonplanar ligands in the malachite green-RNA aptamer complex. Chembiochem Eur J Chem Biol 5(1):62–72. doi:10.1002/cbic.200300701
19. Grate D, Wilson C (1999) Laser-mediated, site-specific inactivation of RNA transcripts. Proc Natl Acad Sci 96(11):6131–6136. doi:10.1073/pnas.96.11.6131
20. Baugh C, Grate D, Wilson C (2000) 2.8 A crystal structure of the malachite green aptamer. J Mol Biol 301(1):117–128. doi:10.1006/jmbi.2000.3951
21. Stojanovic MN, Kolpashchikov DM (2004) Modular aptameric sensors. J Am Chem Soc 126(30):9266–9270. doi:10.1021/ja032013t
22. Babendure JR, Adams SR, Tsien RY (2003) Aptamers switch on fluorescence of triphenylmethane dyes. J Am Chem Soc 125(48):14716–14717. doi:10.1021/ja037994o